

Quantum Maximum Entropy Inference and Hamiltonian Learning

Minbo Gao^{a,b}, Zhengfeng Ji^{*c}, and Fuchao Wei^c

^a *Institute of Software, Chinese Academy of Sciences, Beijing, China*

^b *University of Chinese Academy of Sciences, Beijing, China*

^c *Department of Computer Science and Technology,
Tsinghua University, Beijing, China*

July 17, 2024

Abstract

Maximum entropy inference and learning of graphical models are pivotal tasks in learning theory and optimization. This work extends algorithms for these problems, including generalized iterative scaling (GIS) and gradient descent (GD), to the quantum realm. While the generalization, known as quantum iterative scaling (QIS), is straightforward, the key challenge lies in the non-commutative nature of quantum problem instances, rendering the convergence rate analysis significantly more challenging than the classical case. Our principal technical contribution centers on a rigorous analysis of the convergence rates, involving the establishment of both lower and upper bounds on the spectral radius of the Jacobian matrix for each iteration of these algorithms. Furthermore, we explore quasi-Newton methods to enhance the performance of QIS and GD. Specifically, we propose using Anderson mixing and the L-BFGS method for QIS and GD, respectively. These quasi-Newton techniques exhibit remarkable efficiency gains, resulting in orders of magnitude improvements in performance. As an application, our algorithms provide a viable approach to designing Hamiltonian learning algorithms.

1 Introduction

Maximum entropy inference is a widely used method in machine learning, particularly in the context of graphical models (McCallum et al., 2000; Kindermann & Snell, 1980; Ackley et al., 1985; Bresler, 2015; Hamilton et al., 2017) and natural language processing (Berger et al., 1996). In graphical models, it is known as the *backward mapping*, the problem of computing the model parameters from the marginal information (Wainwright & Jordan, 2007). The inverse problem of estimating marginal parameters from the model parameters is called the *forward mapping*.

Maximum entropy inference is also a core concept in statistical physics (Jaynes, 1957) known as the Jaynes' principle which links statistical mechanics and information theory. The Hammersley-Clifford theorem establishes that, in the classical case, any positive probability distribution satisfying the local Markov property can be represented as a Gibbs distribution (Lafferty et al., 2001). Hence,

*Corresponding author: jizhengfeng@tsinghua.edu.cn

maximum entropy inference is equivalent to learning the classical Hamiltonian defining the Gibbs distribution (Li & Korb, 2020). In recent years, sample-efficient and time-efficient algorithms with demonstrated effectiveness for specific classical graphical models have emerged (Ravikumar et al., 2010; Bresler, 2015; Hamilton et al., 2017; Klivans & Meka, 2017; Vuffray et al., 2016). However, it is technically non-trivial to extend these classical techniques into the quantum domain (Wiebe et al., 2014a,b; Evans et al., 2019; Wang et al., 2017; Anshu et al., 2021; Amin et al., 2018; Bairey et al., 2019, 2020; Haah et al., 2022; Bakshi et al., 2023) due to the non-commutativity of quantum Hamiltonian terms.

In quantum physics, the maximum entropy inference problem naturally arise when we only have partial local information about a quantum many-body system. Let H_j for $j = 1, 2, \dots, m$ be local observables of, say, an n -qubit quantum system. What the state of the system would likely be given only the local marginal information $\alpha_j = \text{tr}(H_j \rho)$? The Jaynes' principle suggests that we take the state to be the one with the maximum von Neumann entropy, which is always a Gibbs state of the form $\xi_{H(\mu)} = \frac{1}{Z(\mu)} e^{-\beta H(\mu)}$ where $H(\mu) = \sum_{j=1}^m \mu_j H_j$ is a quantum Hamiltonian parameterized by a vector of real numbers $\mu = (\mu_j)_{j=1}^m$. That is, given as input the average values $\alpha = (\alpha_j)_{j=1}^m$ encoding local information, the parameter vector μ of the Hamiltonian is uniquely determined by α and the computation of α from μ is an example of the backward mapping problems.

Maximum entropy problem

$$\begin{aligned} \text{maximize: } & S(\rho) \\ \text{subject to: } & \langle H_j, \rho \rangle = \alpha_j, \\ & \rho \text{ is a density matrix,} \end{aligned}$$

Dual problem

$$\begin{aligned} \text{minimize: } & \ln \text{tr} \exp\left(\sum_j \lambda_j H_j\right) - \lambda \cdot \alpha \\ \text{subject to: } & \lambda_j \in \mathbb{R}. \end{aligned}$$

Figure 1: The maximum entropy problem and its dual problem. Here, $S(\rho) = -\text{tr}(\rho \ln \rho)$ is the von Neumann entropy of ρ .

Algorithms for solving the maximum entropy inference problem include the generalized iterative scaling method (Darroch & Ratcliff, 1972; Della Pietra et al., 1997) which has a rich history of study in statistics and gradient descent and variable metric methods originated from optimization research (Malouf, 2002). In this paper, we study quantum generalizations of both the Generalized Iterative Scaling (GIS) algorithm and quasi-Newton methods for solving the Hamiltonian inference problem. Overall, the paper offers three key contributions. Firstly, we present a convergence rate analysis for both Quantum Iterative Scaling (QIS) and Gradient Descent (GD) algorithms. This is achieved by representing the iteration's Jacobian in a concise and explicit formula, which extends a fundamental result from Liang et al. (2004). Secondly, we establish bounds on the eigenvalues of the Jacobian, proving polynomial convergence of both the QIS and GD algorithms. This contribution represents the main technical novelty of the paper. The non-commutativity of the Hamiltonian terms makes the convergence analysis highly non-trivial and divergent from classical proof techniques. Moreover, the lack of a simple closed-form formula for the derivative of the matrix exponential function, due to non-commutativity, further complicates

the analysis. To address this, we introduce a newly proposed quantum belief propagation method (Lemma C.3) that enables the bounding of eigenvalues of the Hessian of the log-partition function, even in cases where an explicit formula for the Hessian is unavailable. In classical settings, this portion of the proof would typically be more straightforward. Lastly, we investigate two variants of quasi-Newton methods that accelerate the iterative processes for QIS and GD, respectively, resulting in significant performance improvements. In the following, we provide a detailed discussion of these three contributions, highlighting their technical significance and implications.

Explicit Jacobian Formula for Iterations. The QIS algorithm we consider here is a natural quantum counterpart to the GIS algorithm. When the matrices are all diagonal, the QIS algorithm reduces to the GIS algorithm for classical maximum entropy inference. Previous work (Ji, 2022) has shown that the algorithm indeed converges to the correct solution of the maximum entropy problem using the auxiliary function method and matrix inequalities. However, while the auxiliary function method is versatile, it falls short in providing a precise assessment of the algorithms’ convergence rates. To solve this problem, we perform a more tailored analysis of the QIS algorithm’s convergence rate in this paper. In the classical case, a corresponding convergence analysis for the GIS algorithm is detailed in Liang et al. (2004). This classical analysis leverages Ostrowski’s theorem, which bounds the convergence rate of an iterative procedure by the spectral radius of the Jacobian matrix associated with the iteration. Our contribution extends the classical analysis to the quantum setting and addresses the difficulty that the gradient of the exponential function for matrices is much more involved than the classical counterpart. We provide a closed-form formula for the Jacobian of the QIS iteration, generalizing the approach of Liang et al. (2004). The formula has a concise form $\mathbb{1} - P^{-1}L$ where P is a diagonal matrix whose entries are the mean values of operators related to H_j over the Gibbs state and L is the Hessian of the log-partition function. This connection to the Hessian matrix L is crucial for the convergence proof.

The maximum entropy problem has a dual problem, which is an *unconstrained* optimization problem regarding the log-partition function in Figure 1. As a comparison, we consider the gradient descent (GD) algorithm for the dual problem. The Jacobian of the GD update process can be computed as $\mathbb{1} - \eta L$ where L is the Hessian of the log-partition function and η is the step size of GD. In a sense, the Jacobian of the QIS update rule, $\mathbb{1} - P^{-1}L$, can be seen as a mechanism to *adaptively* choose the step size for different directions. This is the main advantage that QIS has over the GD algorithm. Numerical simulations in Figure 2 of Section 6 also show that QIS converges significantly faster than GD.

Upper and Lower Bounds for the Jacobian. As our main technical contribution, we analyze the eigenvalues of the Jacobian matrix by establishing both the lower and upper bounds for them.

First, we prove that all eigenvalues of the Jacobian are non-negative. This result is established by proving an *upper bound* on the Hessian of the log-partition function $L \preceq P$. The main difficulty for proving such a bound arises from the fact that there is no simple explicit formula for the derivative of the matrix exponential function $\frac{d}{ds}e^{H+sV}$ when H and V do not commute. Hastings’s quantum belief propagation (Hastings, 2007) expresses the derivative $\frac{d}{ds}e^{H+sV}$ as the anti-commutator $\{e^{H+sV}, \Phi(V)\}$ for some quantum channel Φ depending on $H + sV$ and is the main technical tool used in many previous works for addressing this difficulty. However, this form of quantum belief propagation is not applicable in our case to prove the inequality because the anti-commutator form only guarantees the Hermitian property of the derivative, while the inequality requires positivity. We propose a modified quantum belief propagation operator (see Lemma C.3) to circumvent the problem. In the modified quantum belief propagation, we express $\frac{d}{ds}e^{H+sV}$ as

$e^{(H+sV)/2}\Psi(V)e^{(H+sV)/2}$ for some quantum channel $\Psi(\cdot)$.

Second, we show that the largest eigenvalue of the Jacobian is bounded away from 1 by making a connection to the strong positivity of the log-partition function proven in [Anshu et al. \(2021\)](#), a *lower bound* on the Hessian of the log-partition function. The upper and lower bounds of the Jacobian together complete the convergence rate analysis of the QIS algorithm by using Ostrowski’s theorem (Theorem B.1). As a corollary, this shows that for local Hamiltonians satisfying certain technical conditions, the backward mapping problem can be reduced to the forward mapping problem efficiently. The forward mapping problem is unfortunately a hard problem in general and one may have to resort to approximate inference methods such as variational inference ([Wainwright & Jordan, 2007](#); [Cranmer et al., 2019](#)) or Markov entropy decomposition ([Globerson & Jaakkola, 2007](#); [Poulin & Hastings, 2011](#))

Accelerations. While the QIS and GD algorithms enjoy provable convergence analysis and are expected to converge in a polynomial number of iterations for local Hamiltonians at constant temperature, it can exhibit sluggish performance in practical scenarios. For classical learning of model parameters, quasi-Newton methods are recommended for solving the maximum entropy inference problems, as suggested in a systematic comparison of classical maximum entropy inference algorithms performed in [Malouf \(2002\)](#). Even though the convergence analysis is usually less established, quasi-Newton methods are usually much faster in practice than iterative scaling and gradient descent algorithms.

In light of this, we investigate two families of quasi-Newton accelerations of the algorithms. The first family of heuristic acceleration is based on the Anderson mixing method ([Anderson, 1965](#)). The Anderson mixing algorithm is a heuristic method for accelerating slow fixed-point iterative algorithms. It can be seamlessly integrated to work with the QIS algorithm as QIS is indeed a fixed-point iteration. The Anderson mixing accelerated QIS algorithm (AM-QIS) has *exactly the same* computational requirement of the QIS algorithm in terms of the oracle access and the type of measurements required on the quantum system. The second family is based on the BFGS method ([Nocedal & Wright, 2006](#); [Yuan, 2015](#)) and in particular the limited memory variant, L-BFGS is applied to the GD algorithm (L-BFGS-GD). In our numerical simulations, we observed that AM-QIS and L-BFGS-GD have comparable performance, usually faster by orders of magnitude than the standard QIS and GD algorithms.

We believe that applying such quasi-Newton heuristics is important for quantum optimization algorithms like the QIS algorithm considered here. While quantum computing offers a promising new paradigm with the potential for substantial speedups in specific problems, the practical construction of large-scale quantum computers is still in its early stages. Current quantum computing technology has limitations in terms of scale and suffers from errors. Hence, quantum computing power remains a scarce and valuable resource. Given this situation, the careful optimization of resources required to solve problems on quantum computers emerges as a critical task. The use of Anderson mixing and BFGS for Hamiltonian inference algorithms and potentially for other fixed-point iterative quantum algorithms represents an attempt to achieve such resource optimization. Notably, this approach is not unique to quantum computing. In fact, the quasi-Newton method, which developed into an important optimization heuristics, was initially developed by W. Davidon while working with early classical computers, which often crashed before producing correct results. In response, he devised faster heuristics to expedite calculations later known as the first quasi-Newton method! Quantum computers are currently in its very early stages. They are unstable and prone to errors just like classical computers in the early days; hence, such heuristic speedups may be critical for numerical quantum algorithms.

2 Preliminary

In this section, we introduce some notations used in this paper. For two real vectors $x, y \in \mathbb{R}^m$, we define $x \cdot y$ as $\sum_{i=1}^m x_i y_i$. We sometimes extend this notation to the case when y is a vector of matrices and write, for example, $\lambda \cdot F$ to mean the summation $\sum_j \lambda_j F_j$. For matrices A, B , define $\langle A, B \rangle = \text{tr}(A^\dagger B)$. We use $A \succeq B$ or $B \preceq A$ to mean $A - B$ is a positive semidefinite matrix. A density matrix ρ is a positive semidefinite matrix of unit trace. The set of density matrices on Hilbert space \mathcal{X} is denoted $\text{D}(\mathcal{X})$.

Suppose \mathcal{X} is a finite-dimensional Hilbert space and f is a real convex function. We use Δ to denote the domain $\text{dom } f$ of f , the interval on which f takes well-defined finite values. Then f extends to all Hermitian operators in $\text{Herm}_\Delta(\mathcal{X})$ as $f(X) = \sum_k f(\lambda_k) \Pi_k$ where $X = \sum_k \lambda_k \Pi_k$ is the spectral decomposition of X . Denote the interior and boundary of Δ as Δ_{int} and $\Delta_{\text{bd}} = \Delta \setminus \Delta_{\text{int}}$ respectively. It is easy to see that the domain of matrix function f is $\text{Herm}_\Delta(\mathcal{X})$, and the interior of the domain is $\text{Herm}_{\Delta_{\text{int}}}(\mathcal{X})$. For a subset S of Hermitian matrices, we use $\text{cl}(S)$ to denote the closure of S .

Given convex function f as above, the Bregman divergence for matrices is $D_f(X, Y) = \text{tr}(f(X) - f(Y) - f'(Y)(X - Y))$, where $X \in \text{Herm}_\Delta(\mathcal{X})$ and $Y \in \text{Herm}_{\Delta_{\text{int}}}(\mathcal{X})$. An important case we focus on in this paper is $f(x) = x \ln x - x$. In this case, the matrix Bregman divergence becomes the Kullback-Leibler divergence $D(X, Y) = \text{tr}(X \ln X - X \ln Y - X + Y)$ defined for non-normalized matrices X, Y . When X, Y are positive semidefinite matrices of trace 1, it recovers the Kullback-Leibler relative entropy $D(X, Y) = \text{tr}(X \ln X - X \ln Y)$. We will need the matrix Bregman-Legendre projection $\mathcal{L}(Y, \Lambda)$ and Bregman-Legendre conjugate $\ell(Y, \Lambda)$ for convex function $f(x) = x \ln x - x$ defined as $\mathcal{L}(Y, \Lambda) = \exp(\ln Y + \Lambda)$, $\ell(Y, \Lambda) = \text{tr} \exp(\ln Y + \Lambda) - \text{tr } Y$. For $Y \propto \mathbb{1}$, $\ell(Y, \Lambda) = \text{tr} \exp(\Lambda)$ and we omit Y and write it as $\ell(\Lambda)$.

In this paper, we consider spin Hamiltonians only and write them as $H = \sum_{j=1}^m H_j$ where H_j 's are local terms acting on at most constant number of neighboring qubits according to certain interaction geometry. For example, a $\sigma_z \otimes \sigma_z$ term acting on the first two qubits is $\sigma_z \otimes \sigma_z \otimes (\mathbb{1}^{\otimes n-2})$ for Pauli operator $\sigma_z = \begin{pmatrix} 1 & 0 \\ 0 & -1 \end{pmatrix}$. We often use $\xi_H = \frac{1}{Z} e^{-\beta H}$ to represent the Gibbs state of the Hamiltonian H for inverse temperature β specified in the context or $\beta = 1$ otherwise. Here $Z = \text{tr} e^{-\beta H}$ is the partition function normalizing the state to have trace 1 and plays an important role in statistical physics and also in our work.

3 Quantum Iterative Scaling

This section presents a version of the Quantum Iterative Scaling (QIS) algorithm and discusses its applications in the Hamiltonian inference problem.

We first introduce some notations used in the following discussions. For a given list of Hermitian matrices $F = (F_j)_{j=1}^m$, define the linear family of quantum states $\mathcal{L}(\rho_0)$ as $\{\rho \succeq 0 \mid \langle F_j, \rho \rangle = \langle F_j, \rho_0 \rangle\}$. Define the exponential family $\mathcal{E}(\sigma_0)$ as $\{\frac{1}{Z} \exp(\ln \sigma_0 + \lambda \cdot F)\}$. We introduce the new notation F_j playing the role of H_j in the previous discussion as we will need certain normalization conditions. In the end, we will choose $F_j = \frac{H_j + \mathbb{1}}{2m}$ so F_j is a scaled linear shift of H_j such that $F_j \succeq 0$ and $\sum_j F_j \preceq \mathbb{1}$.

We note that, in Ji (2022), the algorithms are designed for non-normalized matrices and, therefore, there is no need to explicitly normalize $Y^{(t)}$ in the update. Here, we perform explicit normalization to work with normalized quantum states and their von Neumann entropy. For $Y^{(t)} = \exp(\ln \sigma_0 + \lambda \cdot F)$, the normalization is equivalent to a linear update in the summation of

the exponential function $Y^{(t)} = \exp(\ln \sigma_0 + \lambda \cdot F - \ln Z)$ where $Z = \text{tr } Y^{(t)}$. Hence, we have the following two methods to handle the normalization. The first is to let the algorithm to find the normalization implicitly, and this would require that $\mathbb{1}$ is in the span of the F_j 's. This will be the case if the assumption on F_j is that $\sum_j F_j = \mathbb{1}$. The second is to perform the normalization explicitly as we did in the algorithm. This approach is advantageous as it works for all F_j 's satisfying $\sum_j F_j \preceq \mathbb{1}$ even if $\mathbb{1}$ is not in the span of F_j 's.

An important special case of the algorithm is when $\sigma_0 = \mathbb{1}/d$ and $D(\rho, \sigma_0) = \ln(d) - S(\rho)$ where d is the dimension. Then, the minimization over the linear family is now exactly the maximum entropy problem as in Figure 1 with $H_j = F_j$, $\alpha_j = \langle F_j, \rho_0 \rangle$, and $\lambda_j = -\beta \mu_j$. When all the operators F_j 's are diagonal in the computational basis, the QIS algorithm recovers the GIS algorithm (see e.g. Theorem 5.2 of [Csiszár & Shields \(2004\)](#)).

Require: $\rho_0, \sigma_0 \in D(\mathcal{X})$ such that $D(\rho_0, \sigma_0) < \infty$.

Input: $F = (F_1, F_2, \dots, F_k) \in \text{Pos}(\mathcal{X})^k$ and $\sum_{j=1}^k F_j \preceq \mathbb{1}$.

Output: $\lambda^{(1)}, \lambda^{(2)}, \dots$ such that

$$\lim_{t \rightarrow \infty} D(\rho_0, \mathcal{L}(\sigma_0, \lambda^{(t)} \cdot F)) = \inf_{\lambda \in \mathbb{R}^k} D(\rho_0, \mathcal{L}(\sigma_0, \lambda \cdot F)).$$

- 1: Initialize $\lambda^{(1)} = (0, 0, \dots, 0)$.
- 2: **for** $t = 1, 2, \dots$, **do**
- 3: Compute $Y^{(t)} = \mathcal{L}(\sigma_0, \lambda^{(t)} \cdot F)$.
- 4: **for** $j = 1, 2, \dots, k$ **do**
- 5: $\delta_j^{(t)} = \ln \langle F_j, \rho_0 \rangle - \ln \langle F_j, Y^{(t)} / \text{tr } Y^{(t)} \rangle$.
- 6: **end for**
- 7: Update parameters $\lambda^{(t+1)} = \lambda^{(t)} + \delta^{(t)}$.
- 8: **end for**

Algorithm 1: Quantum iterative scaling algorithm.

To give some intuition behind the QIS algorithm, we define $\xi^{(t)} = Y^{(t)} / \text{tr } Y^{(t)}$ and note that the update in the QIS algorithm is simply $\delta_j = \ln \langle F_j, \rho_0 \rangle - \ln \langle F_j, \xi^{(t)} \rangle$, which is zero when the linear family constraint $\langle F_j, \rho \rangle = \langle F_j, \rho_0 \rangle$ is satisfied by $\rho = \xi^{(t)}$. In this case, the algorithm stops updating λ in the j -th direction as expected. Otherwise, if the difference between the current mean value $\langle F_j, \xi^{(t)} \rangle$ and the target value $\langle F_j, \rho_0 \rangle$ is big, so will be the update δ_j . The algorithm is, in this sense, *adaptive* when compared to algorithms like multiplicative weight update algorithms ([Arora et al., 2012](#)).

The maximum entropy problem has dual program in Figure 1 which is an unconstrained problem. Hence, it is also attractive to work with the dual using the gradient descent method (or corresponding quasi-Newton methods discussed later in the paper). The gradient of the dual objective function is $\frac{\partial}{\partial \lambda_j} (\ln \ell(\lambda \cdot F) - \lambda \cdot \alpha) = \langle F_j, \xi_{\lambda \cdot F} \rangle - \alpha_j$, where $\xi_{\lambda \cdot F}$ is the Gibbs state for Hamiltonian $\lambda \cdot F$. Therefore, in gradient descent, the update in each step is $\eta(\alpha_j - \langle F_j, \xi_{\lambda \cdot F} \rangle)$, where η is the learning rate. This leads to the gradient descent algorithm in Algorithm 2.

The QIS algorithm generally outperforms the bare-bones GD algorithm and avoids the problem of choosing the step size completely. Consider the update of the QIS algorithm $\ln \alpha_j - \ln \langle F_j, \xi_{\lambda \cdot F} \rangle$, and the update of the GD algorithm $\eta(\alpha_j - \langle F_j, \xi_{\lambda \cdot F} \rangle)$. For α_j and $\langle F_j, \xi_{\lambda \cdot F} \rangle$ in $(0, 1]$, the QIS update is more aggressive than the dual gradient descent for learning rate $\eta \leq 1$ while still guarantees the convergence. This effect is more evident when the two numbers α_j and $\langle F_j, \xi_{\lambda \cdot F} \rangle$

Require: $\rho_0, \sigma_0 \in \mathcal{D}(\mathcal{X})$ such that $D(\rho_0, \sigma_0) < \infty$.

Input: $F = (F_1, F_2, \dots, F_k) \in \text{Pos}(\mathcal{X})^k$ and $\sum_{j=1}^k F_j \preceq \mathbb{1}$.

Output: $\lambda^{(1)}, \lambda^{(2)}, \dots$ such that

$$\lim_{t \rightarrow \infty} D(\rho_0, \mathcal{L}(\sigma_0, \lambda^{(t)} \cdot F)) = \inf_{\lambda \in \mathbb{R}^k} D(\rho_0, \mathcal{L}(\sigma_0, \lambda \cdot F)).$$

- 1: Initialize $\lambda^{(1)} = (0, 0, \dots, 0)$.
- 2: **for** $t = 1, 2, \dots$, **do**
- 3: Compute $Y^{(t)} = \mathcal{L}(\sigma_0, \lambda^{(t)} \cdot F)$.
- 4: **for** $j = 1, 2, \dots, k$ **do**
- 5: $\delta_j^{(t)} = \eta \langle F_j, \rho_0 \rangle - \eta \langle F_j, Y^{(t)} / \text{tr } Y^{(t)} \rangle$.
- 6: **end for**
- 7: Update parameters $\lambda^{(t+1)} = \lambda^{(t)} + \delta^{(t)}$.
- 8: **end for**

Algorithm 2: Gradient descent algorithm for Kullback-Leibler divergence minimization.

are small, which holds in most applications. We will later see that choosing an appropriate learning rate will improve the performance of the GD algorithm considered in Section 4, but it is still less efficient compared to QIS.

4 Convergence Rate

In this section, we analyze the geometric convergence rate for the QIS algorithm in Algorithm 1 for the case when $\sigma_0 = \mathbb{1}/d$. As a comparison, we will also analyze the convergence rate of the GD algorithm (Algorithm 2).

We will come across several matrices which are defined here for later references. For λ and F , we define the corresponding Gibbs state as $\xi = \frac{\exp(\lambda \cdot F)}{\text{tr } \exp(\lambda \cdot F)}$, and for an operator O , we use $\langle O \rangle = \text{tr}(O\xi)$ to mean the average value of O with respect to ξ . Define diagonal matrix $P = \sum_j \langle F_j \rangle |j\rangle\langle j|$. Finally, define L to be the Hessian of the log-partition function $\ln \text{tr } \exp(\lambda \cdot F)$ with λ as the variables.

We have the following two results regarding the QIS and GD algorithms respectively, proved in Appendix B.

Theorem 4.1. *The Jacobian of the iterative update map $\lambda^{(t)} \mapsto \lambda^{(t+1)}$ of Algorithm 1 for $\sigma_0 = \mathbb{1}/d$ is given by $\mathbb{1} - P^{-1}L$ for P and L defined above with $\lambda = \lambda^{(t)}$.*

Theorem 4.2. *The Jacobian of the iterative update map $\lambda^{(t)} \mapsto \lambda^{(t+1)}$ of Algorithm 2 is given by $\mathbb{1} - \eta L$ where L is the Hessian of the log-partition function defined above.*

By the Ostrowski theorem stated in Theorem B.1, the geometric convergence rate of the QIS algorithm is, therefore, governed by the spectral radius of the Jacobian $\mathbb{1} - P^{-1}L$. Hence, we need to prove bounds on the spectral radius. In Anshu et al. (2021), a non-trivial lower bound on L is proved (see Theorem C.6), giving an upper bound of the spectral radius. To prove the lower bound, will need the following result proved in Appendix C.

Theorem 4.3. *Let P and L be matrices defined above. We have $L \preceq P$.*

We are now able to state the convergence rate of the QIS and GD algorithms.

Theorem 4.4. *For Hamiltonian $H = \sum_{j=1}^m \mu_j H_j$ where conditions of Theorem C.6 are satisfied and H_j are traceless terms with norm $\|H_j\| \leq 1$, the QIS algorithm with $F_j = \frac{\mathbb{1} + H_j}{2m}$ and the GD algorithm with the same choices of F_j and $\eta = m$ solve the Hamiltonian inference problem with geometric convergence rate $1 - \Omega\left(\frac{1}{m^2}\right)$.*

Proof of Theorem 4.4. We consider the QIS algorithm first, which is the more difficult case. By Theorem 4.1, $J_{\text{QIS}} = \mathbb{1} - P^{-1}L$. Hence, we can bound the spectral radius as

$$\begin{aligned} r(J_{\text{QIS}}) &= r(\mathbb{1} - P^{-1}L) \\ &= r(\mathbb{1} - L^{1/2}P^{-1}L^{1/2}) \\ &= \left\| \mathbb{1} - L^{1/2}P^{-1}L^{1/2} \right\| \end{aligned}$$

Here, the second line follows from the fact that AB and BA have the same set of eigenvalues and the third step follows as $L^{1/2}P^{-1}L^{1/2}$ is Hermitian. By definition, P is a diagonal matrix whose (j, j) -th entry is $\langle F_j, \xi \rangle = \left\langle \frac{\mathbb{1} + H_j}{2m}, \xi \right\rangle \leq 1/m$. Theorem 4.3 then implies that $\mathbb{1} - P^{-1}L$ has eigenvalues in $[0, 1]$ and

$$r(J_{\text{QIS}}) = 1 - \lambda_{\min}(L^{1/2}P^{-1}L^{1/2}) \leq 1 - m\lambda_{\min}(L). \quad (1)$$

The Hamiltonian is $H(\mu) = \sum_j \mu_j (2mF_j - \mathbb{1})$. Define $\lambda_j = 2m\mu_j$, and $\tilde{H}(\lambda) = \sum_j \lambda_j F_j$. We have $\tilde{H}(\lambda) = H(\mu) + \mu_{\Sigma} \mathbb{1}$ where $\mu_{\Sigma} = \sum_j \mu_j = \sum_j \lambda_j / (2m)$. We compute

$$\begin{aligned} L_{j,k} &= \frac{\partial^2 \ln \text{tr} \exp(\lambda \cdot F)}{\partial \lambda_j \partial \lambda_k} \\ &= \frac{\partial^2 \ln \text{tr} \exp(\lambda \cdot F)}{\partial \mu_j \partial \mu_k} \frac{\partial \mu_j}{\partial \lambda_j} \frac{\partial \mu_k}{\partial \lambda_k} \\ &= \frac{1}{4m^2} \frac{\partial^2 (\ln \text{tr} \exp(H(\mu)) + \sum_j \mu_j)}{\partial \mu_j \partial \mu_k} \\ &= \frac{1}{4m^2} \nabla_{\mu}^2 \ln \text{tr} \exp(H(\mu)). \end{aligned}$$

By Theorem C.6, we have $\lambda_{\min}(L) \geq \Omega\left(\frac{1}{m^3}\right)$. Together with Equation (1), this completes the proof using Theorem B.1.

By a similar calculation, we can prove the claim for the GD algorithm. \square

The above analysis shows that the QIS algorithm has a better geometric convergence rate even if we set $\eta = m$ in the GD algorithm. Numerical simulations in Section 6 also confirm this observation. In some sense, the QIS algorithm is an adaptive gradient descent that can automatically choose the appropriate learning rate for different dimensions as $\langle F_j \rangle$ may differ for each j .

5 Acceleration by Quasi-Newton Methods

The convergence analysis in Section 4 is of theoretical interest but polynomial convergence proved there is usually not enough for practical applications. In this section, we explore the application of quasi-Newton methods, which can significantly improve the efficiency of the adaptive learning

algorithms considered in Section 3. In particular, we study two families of methods, the Anderson mixing (Anderson, 1965) method and the BFGS method (Nocedal & Wright, 2006).

Anderson mixing (abbreviated as AM in the following) is a widely used method employed in numerical and computational mathematics to accelerate the convergence of fixed-point iterations. It particularly excels in scenarios where traditional iterative methods may converge slowly or struggle to find solutions efficiently. The essence of the Anderson mixing algorithm lies in its ability to dynamically combine and update a finite set of historical iterates. It adaptively selects a linear combination of these historical iterates, leveraging the past information to guide the algorithm toward convergence more effectively. This technique finds applications in various scientific and engineering domains, including quantum chemistry (Garza & Scuseria, 2012), machine learning (Sun et al., 2021), and solving complex systems of equations (Brezinski et al., 2022), where it often delivers substantial acceleration in computational tasks.

Applying the Anderson mixing method to the Hamiltonian inference problem, specifically to the Quantum Iterative Scaling (QIS) algorithm, is straightforward due to the inherent nature of QIS as a fixed-point iterative update algorithm. The Anderson-accelerated QIS (AM-QIS) algorithm combines both the QIS iterative step and simple classical processing, so it has exactly the same requirement as the standard QIS algorithm for the oracle access to the Gibbs state or the average values. Since the fixed-point map $g(x)$ in QIS iteration is a contraction, we can set the mixing parameter $\beta_t \equiv 1$ defined in Appendix D and the convergence of AM-QIS follows from the results in Toth & Kelley (2015). We also use the Barzilai-Borwein (BB) method (Barzilai & Borwein, 1988) for choosing the mixing parameter which turns out to be effective and provides further accelerations.

The BFGS method and the limited memory variant L-BFGS are the most influential among many quasi-Newton methods. They are the recommended choice for learning graphical models in the classical machine learning literature Malouf (2002). The BFGS method works with an unconstrained optimization problem $\min_{x \in \mathbb{R}^n} f(x)$. The update in the BFGS algorithm has the form $x_{k+1} = x_k - \eta_k H_k \nabla f(x_k)$, where η_k is the step size which can usually be found by line search, and H_k is a matrix that is updated iteratively during the execution of the algorithm. We consider both a fixed choice or the BB method for the initial approximation of the inverse Hessian H_0 for a fair comparison with AM. The application of BFGS methods to our problem is also straightforward as the dual problem is an unconstrained optimization problem.

AM and BFGS have different application scenarios. AM is an acceleration method for solving fixed-point problems and the approximation G_t of the inverse Jacobian matrix is generally not symmetric. In contrast, BFGS is an optimization method and constructs a symmetric approximation H_t for the inverse Hessian matrix. Since an optimization problem can usually be recast as a fixed-point problem, AM also applies to solving optimization problems. However, BFGS may be more efficient in some cases due to the maintained symmetry structure compared with AM.

6 Experiments

We conducted numerical simulations to assess the comparative efficiency of four approaches: the standard QIS, the standard GD algorithm, AM-QIS, and the L-BFGS-GD algorithm applied to the dual problem. The Linux workstation we used for the numerical experiment has a 16-core CPU (Intel(R) Xeon(R) Platinum 8369HB CPU @ 3.30GHz) and 64GB of memory.

In the experimental setup, we adopted a method involving generating random Gibbs states for random local Hamiltonians, represented as $H = \sum_j \lambda_j H_j$. Here, the local terms, denoted as H_j , consist of tensor products of local Pauli operators, and the λ_j parameters are the values to be

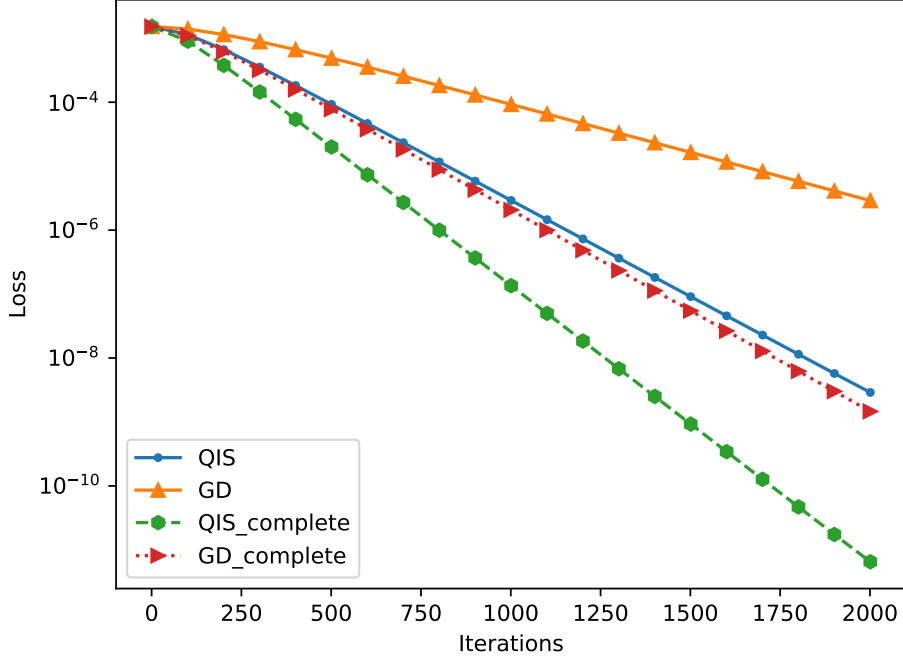


Figure 2: Comparison of QIS and GD algorithms. The loss is measured by the error in the objective function of the maximum entropy problem.

learned. These Hamiltonians were then utilized to create Gibbs states $\xi_H = \frac{1}{Z} e^{-\beta H}$. We feed the Gibbs states and their corresponding local average values $\alpha_j = \langle H_j \otimes \mathbb{1}, \xi_H \rangle$ to the algorithms. In this way, we know the ground truth about the values of λ_j 's and the objective value of the optimization programs in Figure 1, and we choose to evaluate the algorithms' performance by the error compared with the true objective value.

The results are summarized in Figures 2 and 3. In Figure 2, we compare the performance of QIS and GD algorithms. We can see that QIS algorithm is more efficient than GD algorithm regardless of whether we ensure the completeness $\sum F_j = 1$ or not. In Figure 3, we compare the performance of AM-QIS and L-BFGS-GD, both with and without the Barzilai-Borwein method. We can see that AM-QIS and L-BFGS-GD are comparable in general. The standard QIS algorithm typically required approximately 1500 iterations to achieve an error level of $10^{-6} \sim 10^{-8}$ (measured using the objective function of the maximum entropy problem). In contrast, the AM-QIS and L-BFGS-GD algorithms achieved the same accuracy with only about 8 (or 20) iterations with (or without) BB, showcasing a remarkable speedup of two orders of magnitude. The efficiency of the AM-QIS algorithm is stable and does not change much when the Hamiltonian is normalized and completed, while the efficiency of L-BFGS-GD algorithm (in Section 6) is observed to be sensitive in this regard.

7 Discussions

In this study, we considered adaptive learning algorithms for the Hamiltonian inference problem. We examined the convergence of the quantum iterative scaling algorithm (QIS) and the gradient

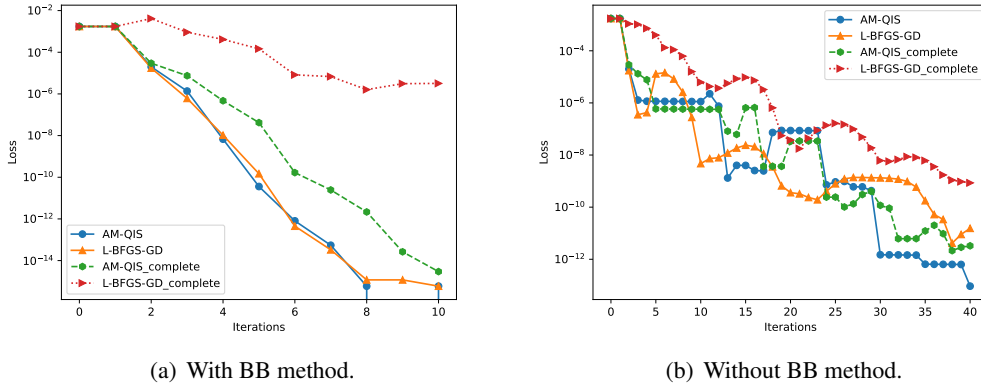


Figure 3: Comparisons of the AM-QIS and L-BFGS-GD algorithms. The Section 6 on the left uses the Barzilai-Borwein method to choose the step size and Section 6 on the right uses fixed step size. The dotted (red) and dashed (green) lines represent the performance of the algorithms when the input Hamiltonian terms are complete satisfying $\sum_j F_j = \mathbb{1}$.

descent (GD) algorithm for the dual problem. Furthermore, two quasi-Newton methods AM-QIS and L-BFGS-GD are proposed.

The QIS algorithm iteratively updates the Hamiltonian parameters adaptively by comparing $\langle H_j \otimes \mathbb{1}, \xi_{H(\lambda)} \rangle$ and the target value α_j . Therefore it requires the ability to prepare $\xi_{H(\lambda)}$ for the trial parameter λ or estimate the local information of the state. This is generally a computationally demanding assumption, but if the physical system has exponentially decaying correlation and satisfy certain Markov property, the preparation of the Gibbs state or its local observations could be efficient (Brandão & Kastoryano, 2019; Kuwahara et al., 2020). Furthermore, the issue may be solved or mitigated by combining quantum belief propagation algorithms proposed in Hastings (2007); Leifer & Poulin (2008); Poulin & Hastings (2011) which present possible ways of computing the value $\langle H_j \otimes \mathbb{1}, \xi_{H(\lambda)} \rangle$ approximately without generating the full Gibbs state, thereby removing the use of the adaptive Gibbs oracle. We leave the exploration of this possibility as future work.

In the proof of the upper bound of the Hessian of the log-partition function, we developed a modified quantum belief propagation technique, which may be of independent interest. It is an interesting problem to find more applications of this new tool.

References

- Ackley, D. H., Hinton, G. E., and Sejnowski, T. J. A learning algorithm for Boltzmann machines. *Cognitive Science*, 9(1):147–169, 1985.
- Amin, M. H., Andriyash, E., Rolfe, J., Kulchytskyy, B., and Melko, R. Quantum Boltzmann Machine. *Physical Review X*, 8(2):021050, 2018.
- Anderson, D. G. Iterative Procedures for Nonlinear Integral Equations. *Journal of the ACM*, 12(4): 547–560, 1965.
- Anshu, A., Arunachalam, S., Kuwahara, T., and Soleimanifar, M. Sample-efficient learning of interacting quantum systems. *Nature Physics*, pp. 1–5, 2021.
- Arora, S., Hazan, E., and Kale, S. The Multiplicative Weights Update Method: a Meta-Algorithm and Applications. *Theory of Computing*, 8(6):121–164, 2012.
- Bairey, E., Arad, I., and Lindner, N. H. Learning a Local Hamiltonian from Local Measurements. *Physical Review Letters*, 122(2):020504, 2019.
- Bairey, E., Guo, C., Poletti, D., Lindner, N. H., and Arad, I. Learning the dynamics of open quantum systems from their steady states. *New Journal of Physics*, 22(3):032001, 2020.
- Bakshi, A., Liu, A., Moitra, A., and Tang, E. Learning quantum Hamiltonians at any temperature in polynomial time. arXiv:2310.02243, 2023.
- Barzilai, J. and Borwein, J. M. Two-Point Step Size Gradient Methods. *IMA Journal of Numerical Analysis*, 8(1):141–148, 1988.
- Berger, A. L., Della Pietra, S. A., and Della Pietra, V. J. A Maximum Entropy Approach to Natural Language Processing. *Computational Linguistics*, 22(1):39–71, 1996.
- Brandão, F. G. S. L. and Kastoryano, M. J. Finite Correlation Length Implies Efficient Preparation of Quantum Thermal States. *Communications in Mathematical Physics*, 365(1):1–16, 2019.
- Bresler, G. Efficiently Learning Ising Models on Arbitrary Graphs. In *Proceedings of the forty-seventh annual ACM symposium on Theory of Computing*, STOC ’15, pp. 771–782, New York, NY, USA, 2015. Association for Computing Machinery.
- Brezinski, C., Cipolla, S., Redivo-Zaglia, M., and Saad, Y. Shanks and Anderson-type acceleration techniques for systems of nonlinear equations. *IMA Journal of Numerical Analysis*, 42(4): 3058–3093, 2022.
- Cranmer, K., Golkar, S., and Pappadopulo, D. Inferring the quantum density matrix with machine learning, 2019.
- Csiszár, I. and Shields, P. C. Information Theory and Statistics: A Tutorial. *Foundations and Trends® in Communications and Information Theory*, 1(4):417–528, 2004.
- Darroch, J. N. and Ratcliff, D. Generalized Iterative Scaling for Log-Linear Models. *Annals of Mathematical Statistics*, 43(5):1470–1480, 1972.
- Davidon, W. C. Variable Metric Method for Minimization. *SIAM Journal on Optimization*, 1(1): 1–17, 1991.

- Della Pietra, S., Della Pietra, V., and Lafferty, J. [Inducing features of random fields](#). *IEEE Transactions on Pattern Analysis and Machine Intelligence*, 19(4):380–393, 1997.
- Evans, T. J., Harper, R., and Flammaria, S. T. [Scalable Bayesian Hamiltonian learning](#), 2019.
- Fang, H.-r. and Saad, Y. [Two classes of multisecond methods for nonlinear acceleration](#). *Numerical Linear Algebra with Applications*, 16(3):197–221, 2009.
- Garza, A. J. and Scuseria, G. E. [Comparison of self-consistent field convergence acceleration techniques](#). *The Journal of Chemical Physics*, 137(5):054110, 2012.
- Globerson, A. and Jaakkola, T. [Approximate inference using conditional entropy decompositions](#). In *Proceedings of the Eleventh International Conference on Artificial Intelligence and Statistics*, pp. 131–138. PMLR, 2007.
- Haah, J., Kothari, R., and Tang, E. [Optimal learning of quantum Hamiltonians from high-temperature Gibbs states](#). In *2022 IEEE 63rd Annual Symposium on Foundations of Computer Science (FOCS)*, pp. 135–146, 2022.
- Hamilton, L., Koehler, F., and Moitra, A. [Information Theoretic Properties of Markov Random Fields, and their Algorithmic Applications](#). In *Advances in Neural Information Processing Systems*, volume 30. Curran Associates, Inc., 2017.
- Hastings, M. B. [Quantum belief propagation: An algorithm for thermal quantum systems](#). *Physical Review B*, 76(20):201102, 2007.
- Jaynes, E. T. [Information Theory and Statistical Mechanics](#). *Physical Review*, 106(4):620–630, 1957.
- Ji, Z. [Classical and quantum iterative optimization algorithms based on matrix Legendre-Bregman projections](#). arXiv:2209.14185, 2022.
- Kindermann, R. and Snell, J. L. *Markov random fields and their applications*. Number 1 in Contemporary mathematics. American mathematical society, Providence, 1980.
- Klivans, A. and Meka, R. [Learning Graphical Models Using Multiplicative Weights](#). In *2017 IEEE 58th Annual Symposium on Foundations of Computer Science (FOCS)*, pp. 343–354, 2017.
- Kuwahara, T., Kato, K., and Brandão, F. G. S. L. [Clustering of Conditional Mutual Information for Quantum Gibbs States above a Threshold Temperature](#). *Physical Review Letters*, 124(22):220601, 2020.
- Lafferty, J. D., McCallum, A., and Pereira, F. C. N. [Conditional Random Fields: Probabilistic Models for Segmenting and Labeling Sequence Data](#). In *Proceedings of the Eighteenth International Conference on Machine Learning, ICML '01*, pp. 282–289, San Francisco, CA, USA, 2001. Morgan Kaufmann Publishers Inc.
- Leifer, M. S. and Poulin, D. [Quantum Graphical Models and Belief Propagation](#). *Annals of Physics*, 323(8):1899–1946, 2008.
- Li, Y. and Korb, K. B. [Learning Graphical Models](#). In Phung, D., Webb, G. I., and Sammut, C. (eds.), *Encyclopedia of Machine Learning and Data Science*, pp. 1–10. Springer US, New York, NY, 2020.

- Liang, G., Yu, B., and Taft, N. [Maximum entropy models: convergence rates and applications in dynamic system monitoring](#). In *International Symposium on Information Theory, 2004. ISIT 2004. Proceedings.*, pp. 168–174, 2004.
- Liu, D. C. and Nocedal, J. [On the limited memory BFGS method for large scale optimization](#). *Mathematical Programming*, 45(1):503–528, 1989.
- Malouf, R. [A comparison of algorithms for maximum entropy parameter estimation](#). In *proceeding of the 6th conference on Natural language learning - COLING-02*, volume 20, pp. 1–7, 2002.
- McCallum, A., Freitag, D., and Pereira, F. C. N. [Maximum Entropy Markov Models for Information Extraction and Segmentation](#). In *Proceedings of the Seventeenth International Conference on Machine Learning, ICML '00*, pp. 591–598, San Francisco, CA, USA, 2000. Morgan Kaufmann Publishers Inc.
- Nocedal, J. and Wright, S. J. *Numerical optimization*. Springer series in operations research. Springer, New York, 2nd ed edition, 2006.
- Ostrowski, A. M. *Solution of Equations and Systems of Equations*. Academic Press, 2nd edition, 1966.
- Poulin, D. and Hastings, M. B. [Markov Entropy Decomposition: A Variational Dual for Quantum Belief Propagation](#). *Physical Review Letters*, 106(8):080403, 2011.
- Qiskit, T. [Qiskit: An open-source framework for quantum computing](#), 2023.
- Ravikumar, P., Wainwright, M. J., and Lafferty, J. D. [High-dimensional Ising model selection using \$\ell_1\$ -regularized logistic regression](#). *The Annals of Statistics*, 38(3):1287–1319, 2010.
- Sun, K., Wang, Y., Liu, Y., Zhao, Y., Pan, B., Jui, S., Jiang, B., and Kong, L. [Damped Anderson Mixing for Deep Reinforcement Learning: Acceleration, Convergence, and Stabilization](#). In *Advances in Neural Information Processing Systems*, volume 34, pp. 3732–3743. Curran Associates, Inc., 2021.
- Toth, A. and Kelley, C. T. [Convergence Analysis for Anderson Acceleration](#). *SIAM Journal on Numerical Analysis*, 53(2):805–819, 2015.
- Vuffray, M., Misra, S., Lokhov, A., and Chertkov, M. [Interaction Screening: Efficient and Sample-Optimal Learning of Ising Models](#). In *Advances in Neural Information Processing Systems*, volume 29. Curran Associates, Inc., 2016.
- Wainwright, M. J. and Jordan, M. I. [Graphical Models, Exponential Families, and Variational Inference](#). *Foundations and Trends® in Machine Learning*, 1(1–2):1–305, 2007.
- Wang, J., Paesani, S., Santagati, R., Knauer, S., Gentile, A. A., Wiebe, N., Petruzzella, M., O’Brien, J. L., Rarity, J. G., Laing, A., and Thompson, M. G. [Experimental quantum Hamiltonian learning](#). *Nature Physics*, 13(6):551–555, 2017.
- Wiebe, N., Granade, C., Ferrie, C., and Cory, D. [Quantum Hamiltonian learning using imperfect quantum resources](#). *Physical Review A*, 89(4):042314, 2014a.
- Wiebe, N., Granade, C., Ferrie, C., and Cory, D. G. [Hamiltonian Learning and Certification Using Quantum Resources](#). *Physical Review Letters*, 112(19):190501, 2014b.

Yuan, Y.-X. **Variable Metric Algorithms**. In Engquist, B. (ed.), *Encyclopedia of Applied and Computational Mathematics*, pp. 1515–1519. Springer, Berlin, Heidelberg, 2015.

A Prime and Dual Divergence Minimization Problems

The primal and dual formulation of the maximum entropy program in Figure 1 is a special case of the following duality result between two minimization problems of the Kullback-Leibler divergence given in Figure 4. The duality theorem of Ji (2022), or Jaynes' principle, states that the following two problems have the same minimizer which is the unique intersection point of the linear family $\mathcal{L}(\rho_0)$ and exponential family $\text{cl}(\mathcal{E}(\sigma_0))$ defined in Section 3. When σ_0 is the maximally mixed state $\mathbb{1}/d$, the linear family minimization is the maximum entropy problem and the exponential family minimization is a dual program in Figure 1.

Linear family minimization

$$\begin{aligned} \text{minimize: } & D(X, \sigma_0) \\ \text{subject to: } & X \in \mathcal{L}(\rho_0). \end{aligned}$$

Exponential family minimization

$$\begin{aligned} \text{minimize: } & D(\rho_0, Y) \\ \text{subject to: } & Y \in \mathcal{E}(\sigma_0). \end{aligned}$$

Figure 4: Two optimization problems of the Kullback-Leibler divergence that are dual to each other.

B Proofs for Convergence Rate

This section proves the explicit formulas for the Jacobian matrix of the iterations in QIS and GD algorithms.

Proof of Theorem 4.1. We first prove two identities about the partial derivative of the function ℓ and its natural logarithm.

$$\frac{\partial}{\partial \lambda_{j'}} \ell(\lambda \cdot F) = \langle F_{j'}, \exp(\lambda \cdot F) \rangle, \quad (2)$$

$$\frac{\partial}{\partial \lambda_{j'}} \ln \ell(\lambda \cdot F) = \langle F_{j'}, \xi \rangle, \quad (3)$$

for ξ defined as

$$\xi = \frac{\exp(\lambda \cdot F)}{\text{tr} \exp(\lambda \cdot F)}. \quad (4)$$

In fact, we have

$$\begin{aligned}
\frac{\partial}{\partial \lambda_{j'}} \ell(\lambda \cdot F) &= \frac{\partial}{\partial \lambda_{j'}} \text{tr} \exp(\lambda \cdot F) \\
&= \text{tr} \sum_{k=0}^{\infty} \frac{\partial}{\partial \lambda_{j'}} \frac{(\lambda \cdot F)^k}{k!} \\
&= \text{tr} \sum_{k=1}^{\infty} \sum_{j=0}^{k-1} \frac{(\lambda \cdot F)^{k-j-1} F_{j'} (\lambda \cdot F)^j}{k!} \\
&= \left\langle F_{j'}, \sum_{k=1}^{\infty} \frac{(\lambda \cdot F)^{k-1}}{(k-1)!} \right\rangle \\
&= \langle F_{j'}, \exp(\lambda \cdot F) \rangle,
\end{aligned}$$

where the second line follows from the Taylor expansion of the matrix expansion and the fourth line is by the cyclic property of trace. This proves Equation (2). Similarly, we have

$$\begin{aligned}
\frac{\partial}{\partial \lambda_{j'}} \ln \ell(\lambda \cdot F) &= \frac{1}{\ell(\lambda \cdot F)} \frac{\partial}{\partial \lambda_{j'}} \ell(\lambda \cdot F) \\
&= \frac{1}{\text{tr} \exp(\lambda \cdot F)} \langle F_{j'}, \exp(\lambda \cdot F) \rangle \\
&= \langle F_{j'}, \xi \rangle,
\end{aligned}$$

where the second line follows from Equation (2). This completes the proof of Equation (3).

Now, for $j = 1, 2, \dots, k$, the update in the algorithm is

$$\delta_j = \ln \langle F_j, \rho_0 \rangle - \ln \left\langle F_j, Y^{(t)} / \text{tr} Y^{(t)} \right\rangle.$$

Hence, for $j, j' \in \{1, 2, \dots, k\}$ and ξ defined in Equation (4),

$$\begin{aligned}
\frac{\partial \delta_j}{\partial \lambda_{j'}} &= - \frac{1}{\langle F_j, \xi \rangle} \frac{\partial \langle F_j, \xi \rangle}{\partial \lambda_{j'}} \\
&= - \frac{1}{\langle F_j, \xi \rangle} \frac{\partial}{\partial \lambda_{j'}} \frac{\partial}{\partial \lambda_j} \ln \ell(\lambda \cdot F) \\
&= - P_{j,j}^{-1} L_{j,j'}.
\end{aligned}$$

For the second line, we used Equation (3). Equivalently, the Jacobian matrix

$$\left(\frac{\partial \delta_j}{\partial \lambda_{j'}} \right)_{j,j'} = -P^{-1}L,$$

for matrices P and L defined in the statement of the theorem. The Jacobian J_{QIS} of the QIS iteration can be written as

$$J_{\text{QIS}} = \mathbb{1} + \left(\frac{\partial \delta_j}{\partial \lambda_{j'}} \right)_{j,j'} = \mathbb{1} - P^{-1}L.$$

This completes the proof the theorem. □

Proof of Theorem 4.2. In an iteration of the algorithm, we have

$$\delta_j = \eta \langle F_j, \rho_0 \rangle - \eta \left\langle F_j, Y^{(t)} / \text{tr } Y^{(t)} \right\rangle.$$

The Jacobian J_{GD} of each iteration has (j, j') entry

$$\begin{aligned} & \mathbb{1} - \eta \frac{\partial}{\partial \lambda_{j'}} \langle F_j, \xi \rangle \\ &= \mathbb{1} - \eta \frac{\partial}{\partial \lambda_{j'}} \frac{\partial}{\partial \lambda_j} \ln \text{tr} \exp(\lambda \cdot F) \\ &= \mathbb{1} - \eta L. \end{aligned}$$

This completes the proof. □

We recall a theorem of Ostrowski which we will use to prove the convergence rate by bounding the spectral radius of a Jacobian matrix.

Theorem B.1 (Ostrowski's theorem (Ostrowski, 1966, Chapter 22)). *Assume function f is differentiable at the neighborhood of a fixed point ζ . For an iterative algorithm $\zeta_{t+1} = f(\zeta_t)$. A sufficient condition for ζ to be a point of attraction is the spectral radius $r(J_f) < 1$. Moreover, if ζ is an attraction point, the geometric convergence rate of the iterative algorithm is given by*

$$\limsup_{t \rightarrow \infty} \frac{\|\zeta_{t+1} - \zeta\|}{\|\zeta_t - \zeta\|} = r(J_f).$$

C Bounds on the Hessian Matrix

In this section, we prove the upper bound on the Hessian of the log-partition function.

The proof uses a modified quantum belief propagation. The idea of quantum belief propagation was studied in Hastings (2007) and we give a version of it in the following lemma. It specifies how the matrix exponential function changes with perturbations of the matrix.

Lemma C.1 (Quantum Belief Propagation (Hastings, 2007)). *Suppose $f_\beta(t)$ is the function whose Fourier transform is*

$$\tilde{f}_\beta(\omega) = \frac{\tanh(\beta\omega/2)}{\beta\omega/2}$$

and $H(s) = H + sV$ for $s \in [0, 1]$. Define the quantum belief propagation operator

$$\Phi_{H(s)}(V) = \int_{-\infty}^{\infty} dt f_\beta(t) e^{-iH(s)t} V e^{iH(s)t}.$$

Then

$$\frac{d}{ds} \exp(\beta H(s)) = \frac{\beta}{2} \left\{ \exp(\beta H(s)), \Phi_{H(s)}(V) \right\}.$$

Here, we introduce a modified version of it to prove that if the perturbation is positive semidefinite, then so is the derivative of the matrix exponential function. That is, the modified quantum belief propagation expresses the derivative $\frac{d}{ds} \exp(\beta H(s))$ so that its positivity is obvious for positive V .

The proof uses the Bochner's theorem and we give a simple version of it which suffices for our purpose.

Lemma C.2 (Bochner's Theorem). *A continuous function $f(x)$ on the real line with $f(0) = 1$ is positive-definite if and only if its Fourier transform is a probability measure on \mathbb{R} .*

Lemma C.3. *Suppose g_β is a function whose Fourier transform is*

$$\tilde{g}_\beta(\omega) = \frac{e^{\beta\omega/2} - e^{-\beta\omega/2}}{\beta\omega}$$

and $H(s) = H + sV$ for $s \in [0, 1]$. Define the modified quantum belief propagation operator

$$\Psi_{H(s)}(V) = \int_{-\infty}^{\infty} dt g_\beta(t) e^{-iH(s)t} V e^{iH(s)t}.$$

Then

$$\frac{d}{ds} \exp(\beta H(s)) = \beta \exp\left(\frac{\beta H(s)}{2}\right) \Psi_{H(s)}(V) \exp\left(\frac{\beta H(s)}{2}\right). \quad (5)$$

Furthermore, $g_\beta(t)$ is a probability density function over the real line and $\Psi_{H(s)}$ is a completely positive trace-preserving map.

Proof of Lemma C.3. Consider the spectrum decomposition of $H(s)$ as $H(s) = \sum_j \lambda_j |\psi_j\rangle\langle\psi_j|$.

Using Duhamel's formula, we have

$$\begin{aligned} \frac{d}{ds} \exp(\beta H(s)) &= \int_0^1 dt e^{t\beta H(s)} \left(\frac{d}{ds} \beta H(s) \right) e^{(1-t)\beta H(s)} \\ &= \beta \int_0^1 dt e^{t\beta H(s)} V e^{(1-t)\beta H(s)}. \end{aligned}$$

Hence, the (j, j') -th entry of $\frac{d}{ds} \exp(\beta H(s))$ in the basis of $\{|\psi_j\rangle\}$ is

$$\begin{aligned} \langle\psi_j| \frac{d}{ds} \exp(\beta H(s)) |\psi_{j'}\rangle &= \beta V_{j,j'} \int_0^1 dt e^{t\beta\lambda_j + (1-t)\beta\lambda_{j'}} \\ &= \begin{cases} \frac{e^{\beta\lambda_j} - e^{\beta\lambda_{j'}}}{\lambda_j - \lambda_{j'}} V_{j,j'} & \text{if } \lambda_j \neq \lambda_{j'} \\ \beta e^{\beta\lambda_j} V_{j,j'} & \text{o.w.} \end{cases} \end{aligned} \quad (6)$$

where $V_{j,j'} = \langle\psi_j|V|\psi_{j'}\rangle$.

Now we simplify the right-hand side of Equation (5). By the definition of $\Psi_{H(s)}(V)$, the (j, j') -th entry of $\Psi_{H(s)}(V)$ in the basis $\{|\psi_j\rangle\}$ is

$$\int_{-\infty}^{\infty} dt g_\beta(t) e^{-i\lambda_j t} V_{j,j'} e^{i\lambda_{j'} t} = \tilde{g}_\beta(\lambda_j - \lambda_{j'}) V_{j,j'}.$$

Hence, the (j, j') -th matrix entry of right-hand side in the basis $\{|\psi_j\rangle\}$ can be written as

$$\beta e^{\beta(\lambda_j + \lambda_{j'})/2} \tilde{g}_\beta(\lambda_j - \lambda_{j'}) V_{j,j'} = \begin{cases} \frac{e^{\beta\lambda_j} - e^{\beta\lambda_{j'}}}{\lambda_j - \lambda_{j'}} V_{j,j'} & \text{if } \lambda \neq \lambda_{j'} \\ \beta e^{\beta\lambda_j} V_{j,j'} & \text{o.w.} \end{cases}$$

which is the same as the (j, j') -th entry of the left-hand side by Equation (6). This completes the proof of Equation (5). The fact that $g_\beta(t)$ is a probability density function and the CPTP property of $\Psi_{H(s)}$ follow from the Bochner's theorem applied to g_β and \tilde{g}_β and the fact that $\tilde{g}_\beta(0) = 1$. \square

To derive the bound in Theorem 4.3, we need two related results stated in Theorem C.4 and Lemma C.5 which we now prove.

Define matrices

$$\begin{aligned}\Delta &= \sum_j \frac{\partial \ell(\lambda \cdot F)}{\partial \lambda_j} |j\rangle\langle j|, \\ \Lambda &= \sum_{j,j'} \frac{\partial^2 \ell(\lambda \cdot F)}{\partial \lambda_j \partial \lambda_{j'}} |j\rangle\langle j'|.\end{aligned}$$

Δ is a diagonal matrix and Λ is the Hessian of the partition function $Z = \ell(\lambda \cdot F) = \text{tr} \exp(\lambda \cdot F)$.

Theorem C.4. *For Λ and Δ defined above, we have $\Lambda \preceq \Delta$.*

Proof of Theorem C.4. Choose $H = \ln Y_0 + \lambda \cdot F$, $\beta = 1$, $s = 0$, and $V = F_{j'}$ in Lemma C.3, we have

$$\begin{aligned}\Lambda_{j,j'} &= \left\langle F_j, \frac{\partial}{\partial \lambda_{j'}} \exp(H) \right\rangle \\ &= \left\langle F_j, e^{H/2} \Psi_H(F_{j'}) e^{H/2} \right\rangle \geq 0.\end{aligned}$$

That is, all entries of matrix Λ (in the basis $(|\psi_j\rangle)$) are non-negative.

Next, we prove that $\Delta - \Lambda$ is a diagonally dominant matrix. For all j' , the sum of the j' -th column is

$$\begin{aligned}\Delta_{j',j'} - \sum_j \Lambda_{j,j'} &= \langle F_{j'}, e^H \rangle - \left\langle \sum_j F_j, e^{H/2} \Psi_H(F_{j'}) e^{H/2} \right\rangle \\ &\geq \langle F_{j'}, e^H \rangle - \langle \Psi_H(F_{j'}), e^H \rangle \\ &= \langle F_{j'}, e^H \rangle - \left\langle \int_{-\infty}^{\infty} dt g_1(t) e^{-iHt} F_{j'} e^{iHt}, e^H \right\rangle \\ &= \langle F_{j'}, e^H \rangle - \int_{-\infty}^{\infty} dt g_1(t) \text{Tr}(e^{-iHt} F_{j'} e^{iHt} e^H) \\ &= \langle F_{j'}, e^H \rangle - \int_{-\infty}^{\infty} dt g_1(t) \text{Tr}(F_{j'} e^H) \\ &= \langle F_{j'}, e^H \rangle - \langle F_{j'}, e^H \rangle = 0.\end{aligned}$$

In the above, the inequality follows from $\sum_j F_j \preceq 1$, the positivity of $e^{H/2} \Psi_H(F_{j'}) e^{H/2}$ and the cyclic property of the trace. The fifth line uses the commutativity of e^{iHt} and e^H and the cyclic property of the trace. The last line follows from the fact that $g_1(t)$ is the probability density function by the Bochner's theorem.

The claim in the theorem now follows by the well-known matrix theory result that diagonally dominant matrices are positive semidefinite. \square

Lemma C.5. *For matrices Δ, Λ defined above and $Q = \sum_{j,j'} \langle F_j \rangle \langle F_{j'} \rangle |j\rangle\langle j'|$, we have the following identity*

$$\Lambda = Z(L + Q).$$

Proof. By definition, we have

$$\begin{aligned} L_{j,j'} &= \frac{\partial^2}{\partial \lambda_j \partial \lambda_{j'}} \ln Z \\ &= \frac{1}{Z^2} \left(Z \frac{\partial^2 Z}{\partial \lambda_j \partial \lambda_{j'}} - \frac{\partial Z}{\partial \lambda_j} \frac{\partial Z}{\partial \lambda_{j'}} \right) \\ &= \frac{1}{Z} \Lambda_{j,j'} - \langle F_j \rangle \langle F_{j'} \rangle, \end{aligned}$$

or equivalently $\Lambda = Z(L + Q)$ in the matrix form. \square

We are now ready to prove the main result stated in Theorem 4.3.

Proof of Theorem 4.3. By Lemma C.5, we have

$$L = \frac{\Lambda}{Z} - Q.$$

Hence, Theorem C.4 implies that

$$L = \frac{\Lambda}{Z} - Q \preceq \frac{\Delta}{Z} - Q = P - Q.$$

As Q is outer product of vector $\sum_j \langle F_j \rangle |j\rangle$, it is a rank-1 and positive semidefinite matrix. Therefore, we have

$$L \preceq P - Q \preceq P$$

which completes the proof. \square

Finally, we will also need a lower bound on L , for which we recall a result about the strong convexity of the log-partition function from Anshu et al. (2021).

Theorem C.6 (Theorem 6 of Anshu et al. (2021)). *Let $H(\mu) = \sum_{j=1}^m \mu_j H_j$ be an ℓ -local Hamiltonian over a finite dimensional lattice. For a given inverse temperature β , there are constants $c, c' > 3$ depending on the geometric property of the lattice such that*

$$\nabla_{\mu}^2 \ln \text{tr}(e^{-\beta H(\mu)}) \succeq \frac{e^{-O(\beta^c)} \beta^{c'}}{m} \mathbb{1}.$$

D Discussions on Quasi-Newton Methods

In this section, we give some details of the Anderson mixing method and L-BFGS method.

The Anderson mixing method interpolates history information in order to speed up a fixed-point iteration. More concretely, suppose $g : \mathbb{R}^d \rightarrow \mathbb{R}^d$ is a contraction and we are interested in finding the fix-point $x = g(x)$. The standard fix-point iterative algorithm is to compute $x_{t+1} = g(x_t)$ for $t = 0, 1, 2, \dots$, until a stopping criteria is met. In Anderson mixing, a relatively small history size $m \geq 0$ is chosen and we define $m_t = \min\{m, t\}$. In our numerical implementation, we use $m = 10$. Define the residual $r_t = g(x_t) - x_t$ and two matrices $X_t, R_t \in \mathbb{R}^{d \times m}$ storing the historical information

$$\begin{aligned} X_t &= (\Delta x_{t-m_t}, \Delta x_{t-m_t+1}, \dots, \Delta x_{t-1}), \\ R_t &= (\Delta r_{t-m_t}, \Delta r_{t-m_t+1}, \dots, \Delta r_{t-1}), \end{aligned}$$

where Δ is the forward difference operator and $\Delta x_k = x_{k+1} - x_k$. Then, the Anderson accelerated iteration can be written succinctly as $x_{t+1} = x_t + G_t r_t$ where

$$G_t = \beta_t I - (X_t + \beta_t R_t)(R_t^T R_t)^{-1} R_t^T.$$

Here, β_t is the mixing parameter.

It is pointed out in [Fang & Saad \(2009\)](#) that G_t approximates the inverse of the Jacobian of g and Anderson mixing method can be thought of as a quasi-Newton method satisfying multi-secant equations. We note that there is a matrix inverse in the above formula for G_t which can be implemented using Moore-Penrose pseudo-inverse. For stability and efficiency concerns, we found that the AM algorithms have the best performance in our numerical simulations when using a relative condition number of $1e-7$ in the pseudo-inverse, a cutoff threshold that sets small singular values of the matrix to zero. This is easily implemented by setting the `rcond` parameter of the `pinv` function in `numpy.linalg` package for Python implementations.

The BFGS method is one of the most popular quasi-Newton methods that can be applied to unconstrained optimization problems $\min_{x \in \mathbb{R}^n} f(x)$. It is also known as the variable metric algorithm as first proposed by Davidon ([Davidon, 1991](#); [Yuan, 2015](#)). The algorithm maintains the approximate Hessian H_{k+1} of the optimization problem. The update rule of the algorithm is

$$x_{t+1} = x_t - \eta_t H_t \nabla f(x_t),$$

and the update rule of H_t is

$$H_{t+1} = \left(\mathbb{1} - \frac{s_t y_t^T}{y_t^T s_t} \right) H_t \left(\mathbb{1} - \frac{y_t s_t^T}{y_t^T s_t} \right) + \frac{s_t s_t^T}{y_t^T s_t},$$

where $s_t = x_{t+1} - x_t$, $y_t = \nabla f(x_{t+1}) - \nabla f(x_t)$ and H_0 is a predefined initial approximation of the inverse Hessian matrix. We refer readers to [Nocedal & Wright \(2006\)](#) for a discussion on how the BFGS update is derived. To optimize the memory usage, the limited memory version of BFGS called L-BFGS ([Liu & Nocedal, 1989](#)) is used. Since using line search for choosing η_t can incur additional function evaluations in each iteration, we use $\eta_t \equiv 1$ and only tune H_0 in the numerical simulation.

Both the AM and the BFGS methods employed our numerical simulation can be further strengthened by using a heuristics invented by Barzilai and Borwein ([Barzilai & Borwein, 1988](#)) to choose the β_t in AM and H_0 in BFGS. In AM, we set

$$\beta_t = -\frac{\Delta r_{t-1}^T \Delta x_{t-1}}{\Delta r_{t-1}^T \Delta r_{t-1}},$$

which solves $\min_{\beta} \|\Delta x_{t-1} + \beta \Delta r_{t-1}\|_2$. In BFGS, we set

$$H_0 = \frac{y_{t-1}^T s_{t-1}}{y_{t-1}^T y_{t-1}} \mathbb{1}$$

to be the initialization of the approximate inverse Hessian in the t -th iteration ([Nocedal & Wright, 2006](#), Pages 143 and 178).

E Experimental Details

In this section, we provide details of the numerical experiments.

E.1 Hamiltonian Generation

Three types of Hamiltonians are used in our numerical experiments. These include the Ising family of Hamiltonians, the transversal 2-local Hamiltonians in 1D (Transversal1D), and the 2-local Hamiltonians in 1D (Local1D). The figures in the main text demonstrate the results of the experiments on the Local1D Hamiltonian in 6-qubit system.

Ising Hamiltonian The Ising Hamiltonian is a sum of 2-local terms, which can be written as

$$H = \sum_{i=1}^n a_i \sigma_x^{(i)} + \sum_{i=1}^{n-1} b_i \sigma_z^{(i)} \sigma_z^{(i+1)},$$

where $\sigma_z^{(i)}$ is a Pauli Z operator acting on the i -th qubit. The coefficients a_i and b_i are randomly generated from the standard normal distribution.

Transversal1D Hamiltonian The transversal 1D Hamiltonian is a sum of 2-local terms, and it can be written as

$$H = \sum_{p \in \{x,y,z\}} a_p \sum_{i=1}^n \sigma_p^{(i)} + \sum_{p,q \in \{x,y,z\}} b_{p,q} \sum_{i=1}^n \sigma_p^{(i)} \sigma_q^{(i+1)}.$$

The coefficients a_j and $b_{p,q}$ are randomly generated from the standard normal distribution.

Notice that, in this scenario, there are 12 terms in the Hamiltonian, and each term in the Hamiltonian is a sum of Pauli operators acting on different qubits. Thus, the operator norm of each term is bounded by the number of qubits instead of 1. As a result, in the implementation of our algorithm, we need to normalize the Hamiltonian by dividing the number of qubits.

Local1D Hamiltonian The local 1D Hamiltonian is a sum of 2-local terms, including the Ising Hamiltonian as a special case, and it can be written as

$$H = \sum_{i=1}^n \sum_{p \in \{x,y,z\}} a_{p,i} \sigma_p^{(i)} + \sum_{i=1}^n \sum_{p,q \in \{x,y,z\}} b_{p,q,i} \sigma_p^{(i)} \sigma_q^{(i+1)},$$

where $\sigma^{(i)}$ is a Pauli operator acting on the i -th qubit for $i \leq n$, and $\sigma^{(n+1)}$ is defined as $\sigma^{(n+1)} = \sigma^{(1)}$. The coefficients $a_{p,i}$ and $b_{p,q,i}$ are randomly generated from the standard normal distribution.

E.2 Initialization, Learning Rate, and Stopping Criteria

The initial guess for the parameters in the QIS algorithm and the gradient descent algorithm is set to 0. The learning rate in the gradient descent algorithm is set to the number of terms in the Hamiltonian. In the experiments, we first generate the Hamiltonian and then normalize it by dividing it by the number of qubits. Then, the inverse temperature β is set to 1. Therefore, the optimal solutions and optimal objective values can be directly computed and compared with the results of the algorithms. With these settings, the stopping criteria can be set to the error of the objective value. The stopping criteria for the QIS, gradient descent algorithm, and quasi-Newton accelerations is set to have error at most 10^{-12} . The maximum number of iterations for the quasi-Newton accelerations is set to 40.

	QIS	GD	AM-QIS	L-BFGS-GD
6-qubit-Ising	319	479	7	6
6-qubit-Transversal	1743	2562	5	7
6-qubit-Local	1913	2377	5	8
7-qubit-Ising	370	551	6	6
7-qubit-Transversal	2006	2940	5	7
7-qubit-Local	2236	2721	5	7
8-qubit-Ising	421	623	6	5
8-qubit-Transversal	2267	3311	4	7
8-qubit-Local	2525	3020	5	7

Table 1: Number of steps to achieve 10^{-7} precision for different Hamiltonians.

E.3 Results on Different Hamiltonians

In this section, we provide the results of the numerical experiments on different Hamiltonians. We have conducted experiments on the Ising, Transversal1D, and Local1D Hamiltonians, with different numbers of qubits. The results are shown in the following tables and figures. We first present the results in Table 1 and then provide the figures for each family of Hamiltonians.

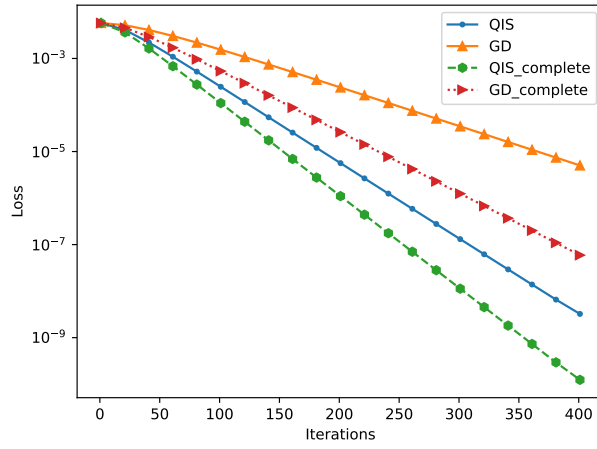
The results of the Ising Hamiltonian are shown in Figure 5 for a 7-qubit system with 13 Hamiltonian terms. In such cases, the QIS algorithm converges to the optimal solution with error 10^{-9} in roughly 400 iterations with less loss than the GD algorithm, while the quasi-Newton methods converge to the optimal solution with similar error in less than 20 iterations.

The results of the Transversal1D Hamiltonian are shown in Figure 6 for a 7-qubit system with 12 terms. In such cases, the QIS algorithm converges to the optimal solution with error 10^{-7} in roughly 1000 iterations with less loss than the GD algorithm, while the quasi-Newton methods converge to the optimal solution with similar error in less than 20 iterations.

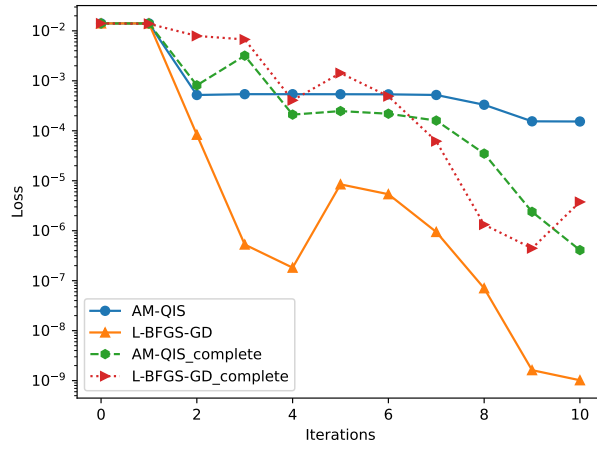
The results of the Local1D Hamiltonian are shown in Figure 7 for a 7-qubit system with 96 terms. In such cases, the QIS algorithm converges to the optimal solution with error 10^{-9} in roughly 2000 iterations with less loss than the GD algorithm, while the quasi-Newton methods converge to the optimal solution with similar error in less than 40 iterations.

E.4 Reproducibility Details

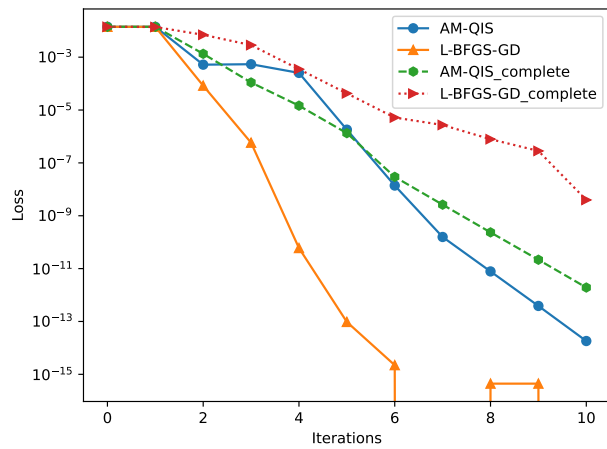
The numerical experiments were conducted using Python 3.11.5 in Python scripts. Running the script requires the following packages: numpy and scipy for linear algebra operations, matplotlib for data visualization, sys for outputting results in txt format, time for measuring the runtime of the algorithm, and Qiskit (Qiskit, 2023) for generating Hamiltonians. For reproducibility, we set the random seed to 100 for QIS and GD, and random seed array from 1 to the number of experiments for quasi-Newton accelerations. The average runtime of the script is less than 6 minutes for systems of five to eight qubits (of dimensions 32×32 to 256×256).



(a) QIS and GD results.

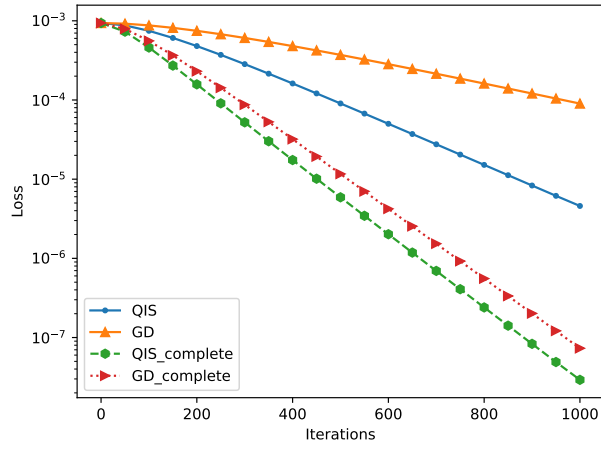


(b) Quasi-Newton methods without BB method.

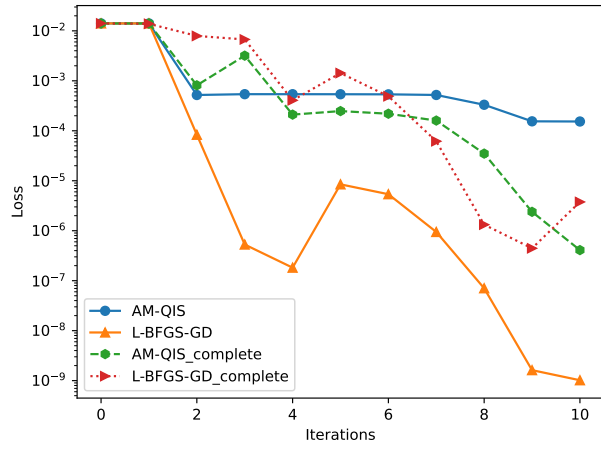


(c) Quasi-Newton methods with BB method.

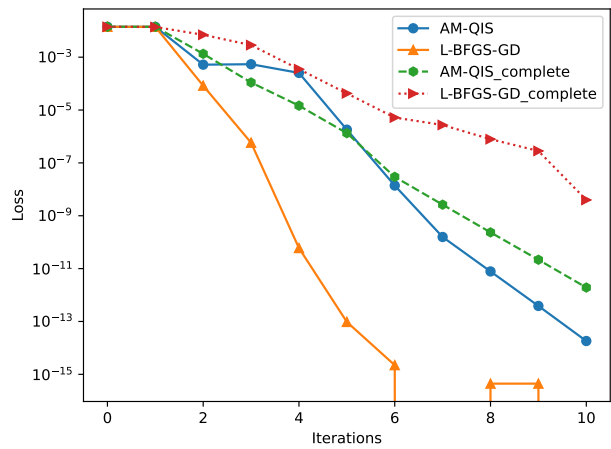
Figure 5: Results of the Ising Hamiltonian for 7 qubits.



(a) QIS and GD results.

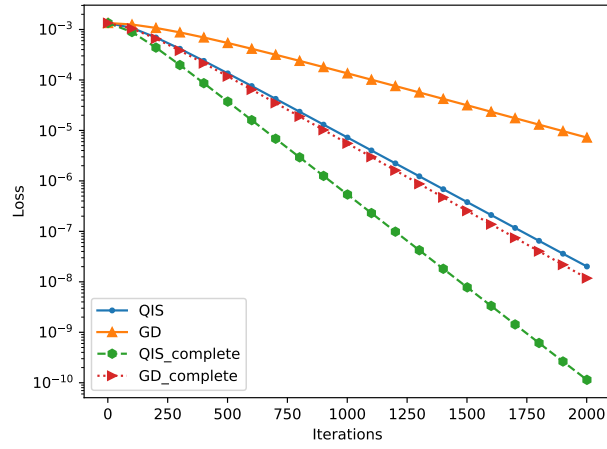


(b) Quasi-Newton methods without BB method.

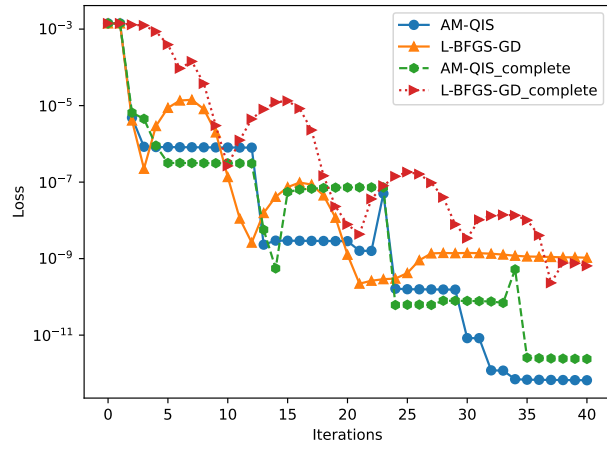


(c) Quasi-Newton methods with BB method.

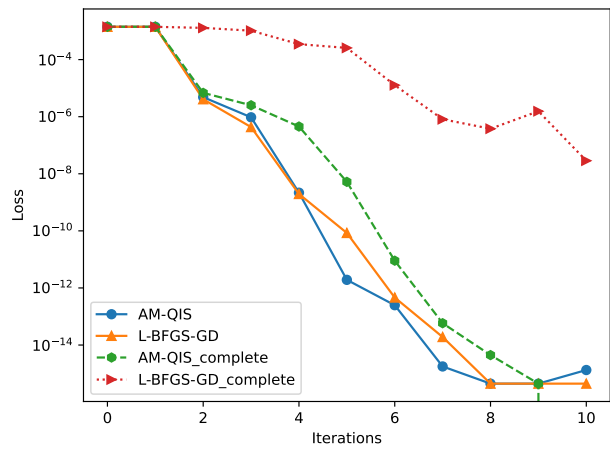
Figure 6: Results of the Transversal1D Hamiltonian for 7 qubits.



(a) QIS and GD results.



(b) Quasi-Newton methods without BB method.



(c) Quasi-Newton methods with BB method.

Figure 7: Results of the Local1D Hamiltonian for 7 qubits.